Acta Cryst. (1978). A**34**, 268–274

A Neutron Investigation of the Low-Temperature Structure of $RbH_3(SeO_3)_2$

BY H. GRIMM* AND W. J. FITZGERALD

Institut Max von Laue–Paul Langevin, BP 156*X*, 38042 *Grenoble CEDEX, France*

(*Received* 4 *March* 1977; *accepted* 12 *October* 1977)

The crystal structure of $RbH_3(SeO_3)_2$ has been determined in the low-temperature phase (space group $P2_1$) with neutron diffraction. The crystal undergoes an improper ferroelectric phase transition at 158 K and the unit cell is doubled below the transition temperature. This transition is induced by the condensation of a soft mode at the Brillouin zone boundary. Imposing the symmetry of the soft-mode eigenvector on the static displacements from the high-temperature positions (space group $P2_12_12_1$) results in a reduction, by a factor of four, of the number of positional parameters required to describe the low-temperature structure. The crystal is constructed of two types of chains consisting of SeO_3 groups connected by hydrogen bonds, and the order parameter for the transition is shown to be the rigid rotations of the SeO_3 tetrahedra belonging to one type of chain. The atomic displacements necessary to produce the observed spontaneous polarization are shown to be too small to be observed in the present experiment, and the precise mechanism responsible for the spontaneous polarization remains unknown.

I. Introduction

The family of crystals belonging to the alkali-metal trihydrogen selenites $AH_3(SeO_3)_2$ has recently been shown to display interesting properties with respect to phase transitions, hydrogen bonding and ferroelectricity (see, for example, Shuvalov, Ivanov, Gordeyeva, & Kirpichnikova, 1969). In many respects the Rb compound is unique within the family. It undergoes a ferroelectric phase transition at about 158 K which is nearly second order. In contrast to other family members, proton ordering seems to play no role in the phase transition, since there is essentially no isotope shift in the transition temperature T_c (Shuvalov *et al.*, 1970) and a positive gradient of T_c with respect to pressure (Gesi, Ozawa & Makita, 1973). A negative gradient is expected for proton ordering since increasing the pressure lowers the barrier between the two proton sites.

The spontaneous polarization of $RbH_3(SeO_3)_2$ is not the order parameter of the phase transition, and the crystal belongs to the group of improper ferroelectrics (Shuvalov *et al.*, 1969). This is indicated by the extremely small value of the spontaneous polarization of 0·013 μC cm^{-2} (Shuvalov *et al.*, 1969) (*cf.* ~5 μC cm^{-2} for KDP) and proved by the observation of a condensing zone-boundary mode (Grimm & Fitzgerald, 1978) which leads to a doubling of the *c* axis. The corresponding superlattice reflections have been shown to exist by Makita & Suzuki (1974) and independently by Aknazarov, Shekhtman & Shuvalov (1974) with X-rays. With neutrons, the temperature dependence of the order parameter, obtained from the superlattice intensities, has been discussed by the present authors (Fitzgerald & Grimm, 1977). However, to our knowledge no attempt has been made to determine the structure of the low-temperature phase. To understand the mechanism responsible for the phase transition it is helpful to know the low-temperature structure. At room temperature the structure of $RbH_3(SeO_3)_2$ has been investigated by Tovbis, Davydova & Simonov (1972) and by Tellgren & Liminga (1973) with X-ray diffraction. The crystal belongs to the orthorhombic space group $P2_12_12_1$ (D_2^4) and contains four formula units per unit cell of dimensions: a = 5·9192 (2), b = 17·9506 (5), c' = 6·2519 (3) Å. In the following we refer to the doubled low-temperature cell with $c = 2c'$. The crystal may be thought of as being built up of two chains running in the **a** and **c** directions. These chains consist of SeO_3 pyramidal groups interlinked by hydrogen bonds. The third hydrogen bond of the molecule connects the two chains thus forming a three-dimensional network (Fig. 2).

The present paper describes the method and the results of a structural analysis of the low-temperature phase of $RbH_3(SeO_3)_2$, obtained with neutron diffraction. This paper is divided into five sections. In § II, the symmetry constraints on the soft-mode eigenvector are investigated (details are presented in the Appendix). This helps to reduce the number of parameters describing the structure of the low-temperature phase. §§ III and IV deal respectively with the experiment and the details of the structure refinement. The results of the refinement are presented and discussed in § V.

---

* Guest scientist on leave from Institut für Festkörperforschung, Kernforschungsanlage, Jülich, Federal Republic of Germany, now returned.

II. Symmetry considerations

Knowing the space group of the high-temperature phase and the wave vector of the soft mode of a second-order displacive phase transformation, one may investigate the transformation properties of the soft-mode eigenvector to gain information about the low-temperature structure. This assumes that the difference between the high and low-temperature structure shows the soft-mode eigenvector symmetry. The validity of this assumption has been proved for many second-order displacive phase transitions. The symmetry operations of space group $P2_12_12_1$ are:

$$x,y,z;\ x+\tfrac{1}{2},-y+\tfrac{1}{2},-z;\ -x,y+\tfrac{1}{2},-z+\tfrac{1}{2};\ -x+\tfrac{1}{2},-y,z+\tfrac{1}{2}. \tag{1}$$

The group of the soft-mode wave vector $\mathbf{k}_{22} = \mathbf{c}^*/2$ contains all four rotational elements R_s of the space group, and has only one two-dimensional representation (Kovalev, 1965),

$$\begin{array}{c|c|c|c|c} & \mathsf{R}_1 & \mathsf{R}_2 & \mathsf{R}_3 & \mathsf{R}_4 \\ \hline \tau(s) & \boldsymbol{\varepsilon} & \boldsymbol{\sigma}_z & -i\boldsymbol{\sigma}_y & \boldsymbol{\sigma}_x \end{array} \tag{2}$$

where

$$\boldsymbol{\sigma}_x = \begin{pmatrix} 0 & 1 \\ 1 & 0 \end{pmatrix} \quad \boldsymbol{\sigma}_y = \begin{pmatrix} 0 & -i \\ i & 0 \end{pmatrix} \quad \boldsymbol{\sigma}_z = \begin{pmatrix} 1 & 0 \\ 0 & -1 \end{pmatrix} \tag{3}$$

and satisfy the relations:

$$\boldsymbol{\sigma}_x^2 = \boldsymbol{\sigma}_y^2 = \boldsymbol{\sigma}^2 = \boldsymbol{\varepsilon};\quad \boldsymbol{\sigma}_x\boldsymbol{\sigma}_y = -\boldsymbol{\sigma}_y\boldsymbol{\sigma}_x = i\boldsymbol{\sigma}_z. \tag{4}$$

This representation means that all $3r$ modes are doubly degenerate for this wave vector because of spatial symmetry. This degeneracy (Levanyuk & Sannikov, 1970) is expected for an improper ferroelectric because otherwise the spontaneous polarization P_s cannot reverse its sign. The reason for this is the quadratic coupling to the order parameter η which in essence is represented by the soft mode eigenvector. Thus, P_s has to be proportional to terms like $\eta_1\eta_2$ or $\eta_1^2-\eta_2^2$ where η_1, η_2 represent the two eigenvectors associated with the degenerate soft-mode eigenvalue. It is clear that a twofold degeneracy is merely the minimum requirement.

An arbitrary basis vector has $3r$ (= 144) complex components and will be written

$$\mathbf{E}(\lambda) = [E_\alpha(K,\kappa,\lambda)] \tag{5}$$

where α denotes the Cartesian component, K labels the 12 atoms of the molecule, κ denotes the molecule created by the κth symmetry operation and λ labels the two degenerate modes. It is understood that $\mathbf{E}(\lambda)$ belongs to the soft mode. Because the symmetry operations applied to $\mathbf{E}(\lambda)$ will not mix atoms of different K, the index K is suppressed in the following and one may think of $\mathbf{E}(\lambda)$ as a 12-component vector ($\kappa = 1\ldots 4$) of the form

$$\mathbf{E}(\lambda) = [\mathbf{D}_1(\lambda), \mathsf{R}_2\mathbf{D}_2(\lambda), \mathsf{R}_3\mathbf{D}_3(\lambda), \mathsf{R}_4\mathbf{D}_4(\lambda)] \tag{5a}$$

where for convenience the components $E_\alpha(\kappa,\lambda)$ are written in the form $\mathsf{R}_\kappa\mathbf{D}_\kappa(\lambda)$.

By means of projection-operator techniques one can reduce the number of independent components of the basis vector (5) with the help of representation (2) as described by Maradudin & Vosko (1968). The essential steps of this somewhat lengthy analysis are given in the Appendix. The result is:

$$\begin{aligned} \mathbf{E}(1) &= \{\mathbf{D}_1, \mathsf{R}_2\mathbf{D}_1, \mathsf{R}_3\mathbf{D}_2, -\mathsf{R}_4\mathbf{D}_2\} \\ \mathbf{E}(2) &= \{\mathbf{D}_2, -\mathsf{R}_2\mathbf{D}_2, \mathsf{R}_3\mathbf{D}_1, \mathsf{R}_4\mathbf{D}_1\} \end{aligned} \tag{6}$$

where $\mathbf{D}_1$ and $\mathbf{D}_2$ are arbitrary, real displacement vectors. Such a pair of displacement vectors has to be defined for each atom K of the molecule. The $\mathbf{D}$ are real owing to time-reversal symmetry. Also, time-reversal symmetry does not produce any further degeneracy for the soft-mode wave vector.

The basis vectors $\mathbf{E}(\lambda)$ do not necessarily represent the eigenvector of the soft mode. One merely may suppose that the low-temperature structure is produced by the condensation of a linear combination $\mathbf{e}(\lambda)$ of the basis vectors,

$$\mathbf{e}(\lambda) = \alpha\mathbf{E}(1) + \beta\mathbf{E}(2). \tag{7}$$

The low-temperature structure is known to be monoclinic with b the unique axis (Shuvalov *et al.*, 1969). This means that the point operation R_3 is conserved in the low-temperature phase. The consequences of this fact are seen from the following list of low-temperature positions $\mathbf{r}_\kappa$ for one kind of atom

$$\left.\begin{aligned} \mathbf{r}_1 &= \mathsf{R}_1(\boldsymbol{\rho}+\mathbf{d}_1) + (0,0,0) \\ \mathbf{r}_2 &= \mathsf{R}_2(\boldsymbol{\rho}+\mathbf{d}_2) + (\tfrac{1}{2},\tfrac{1}{2},0) \\ \mathbf{r}_3 &= \mathsf{R}_3(\boldsymbol{\rho}+\mathbf{d}_3) + (0,\tfrac{1}{2},\tfrac{1}{4}) \\ \mathbf{r}_4 &= \mathsf{R}_4(\boldsymbol{\rho}+\mathbf{d}_4) + (\tfrac{1}{2},0,\tfrac{1}{4}) \\ \mathbf{r}_5 &= \mathsf{R}_1(\boldsymbol{\rho}-\mathbf{d}_1) + (0,0,\tfrac{1}{2}) \\ \mathbf{r}_6 &= \mathsf{R}_2(\boldsymbol{\rho}-\mathbf{d}_2) + (\tfrac{1}{2},\tfrac{1}{2},\tfrac{1}{2}) \\ \mathbf{r}_7 &= \mathsf{R}_3(\boldsymbol{\rho}-\mathbf{d}_3) + (0,\tfrac{1}{2},\tfrac{3}{4}) \\ \mathbf{r}_8 &= \mathsf{R}_4(\boldsymbol{\rho}-\mathbf{d}_4) + (\tfrac{1}{2},0,\tfrac{3}{4}) \end{aligned}\right\} \tag{8}$$

where $\boldsymbol{\rho}$ represents the high-temperature position and the primitive translations are written in terms of the low-temperature cell. The form of (8) expresses the fact that the condensation of a phonon with wave vector $\mathbf{k}_{22} = (0,0,\tfrac{1}{2})$ produces the low-temperature structure (Grimm & Fitzgerald, 1978) since

$$\mathbf{r}_{\kappa+4} = \mathbf{r}_\kappa - 2\,\mathsf{R}_\kappa\boldsymbol{\rho} + (0,0,\tfrac{1}{2}). \tag{9}$$

The screw rotation around the **y** direction $(-x, y+\frac{1}{2}, -z+\frac{1}{4})$ interchanges atoms κ and $\kappa+2$, as can be seen from (8). This gives rise to two possible constraints on the $\mathbf{d}_\kappa$. One has either

$$\mathbf{d}_\kappa = \mathbf{d}_{\kappa+2} \quad \text{or} \quad \mathbf{d}_\kappa = -\mathbf{d}_{\kappa+2}. \tag{10}$$

Application of (10 to (6) and (7) gives $\alpha = \beta$ or $\alpha = -\beta$. Therefore, the soft-mode eigenvector has to be of the form

$$\mathbf{e}(1) = (\mathbf{D}'_1, \mathsf{R}_2\mathbf{D}'_2, \mathsf{R}_3\mathbf{D}'_1, \mathsf{R}_4\mathbf{D}'_2) \tag{11a}$$

$$\mathbf{e}(2) = (\mathbf{D}'_2, \mathsf{R}_2\mathbf{D}'_1, -\mathsf{R}_3\mathbf{D}'_2, -\mathsf{R}_4\mathbf{D}'_1) \tag{11b}$$

where

$$\mathbf{D}'_1 = \mathbf{D}_1 + \mathbf{D}_2 \quad \text{and} \quad \mathbf{D}'_2 = \mathbf{D}_1 - \mathbf{D}_2.$$

The task of obtaining the low-temperature structure by experiment seems at first sight to be difficult because of the high number of atoms per asymmetric unit. The high-temperature structure has already 12 atoms in the asymmetric unit compared with 48 below T_c because of the loss of symmetry and the doubling of the unit cell. However, using the symmetry considerations leading to equation (11) one merely has to determine 24 atomic positions, represented by the $\mathbf{D}'_\kappa$, to describe the low-temperature structure. Equation (11) shows that there will exist two domains in the low-temperature structure, corresponding to the condensation of either $\mathbf{e}(1)$ or $\mathbf{e}(2)$.

III. Experimental

The present experiment was performed at the High-Flux Reactor in Grenoble with the four-circle diffractometer D10 (ILL, 1974). A Cu 200 reflection was used to produce monochromatic neutrons of wavelength $\lambda = 1{\cdot}439$ Å. Excellent crystals, having a mosaic width less than 1′, were grown by H. Zimmerman;* the one used had a volume of approximately 6 mm^3 and a natural habit, with a transmission of 80% corresponding to an effective thickness of the sample of 1 mm and a total scattering of $1{\cdot}8$ cm^{-1}. 1154 reflections were obtained at 112 K, and corrected for background and Lorentz factor. 611 reflections were non-equivalent.

IV. Structure refinement

For the refinement of the structure a short version of the XRAY 70 system, called *XFLS* (Klar, 1975), was used. This least-squares program had to be modified in order to include the effect of domains and the constraints due to equation (11).

There is no chance in such an experiment of separating the reflections of different domains, because the monoclinic angle differs only by approximately 40″ from 90° (Ivanov, Tukhtasunov & Shuvalov, 1970). Therefore, one can either introduce a domain parameter into the refinement program or sum up odd reflections (see below) which are related by $\mathsf{R}_2(C_{2x})$, because this sum is independent of the domain distribution (Fitzgerald & Grimm, 1977). We decided to follow the first possibility because of the better ratio of the number of fitted parameters to the number of observations. Restricting the least-squares fit by unit-weight isotropic extinction correction (Coppens & Hamilton, 1970) and isotropic Debye–Waller factors, the fit gave an R factor of 5%. The refined domain parameter showed the crystal to be entirely in one orientation corresponding to the eigenvector $\mathbf{e}(1)$ (see also Fitzgerald & Grimm, 1977).

The essential features of the phase transformation can be made clear by looking at the difference between the high and low-temperature structures. A pseudo high-temperature structure, in the following referred to as the 'even structure', can be obtained from the present data measured at 112 K by refining the data without the superlattice reflections. This is possible because of the smallness of the atomic displacements $\mathsf{R}_\kappa\mathbf{d}_\kappa$ from the high-temperature positions. The structure factor can be written

$$F(\mathbf{Q}) = \sum_{K=1}^{12} b_K(\mathbf{Q}) f_K(\mathbf{Q}) \tag{12}$$

where $\mathbf{Q}$ represents a reciprocal-lattice vector, $b_K(\mathbf{Q})$ represents the scattering length and the Debye–Waller factor.

$$f(\mathbf{Q}) = \sum_{\kappa=1}^{8} \exp(i\mathbf{Q}\mathbf{r}_\kappa) \tag{13}$$

represents the contribution of the Kth type of atom to the structure factor. Inserting (8) into (13) one obtains for 'even' reflections:

$$f(h,k,2l) = 2\sum_{\kappa=1}^{4} \exp[i\mathbf{Q}(\mathsf{R}_\kappa\boldsymbol{\rho} + \mathbf{V}'_\kappa)]\cos Q\mathsf{R}_\kappa\mathbf{d}_\kappa \tag{14}$$

and for 'odd' reflections:

$$f(h,k,2l+1) = 2i\sum_{\kappa=1}^{4} \exp[i\mathbf{Q}(\mathsf{R}_\kappa\boldsymbol{\rho} + \mathbf{V}'_\kappa)]\sin Q\mathsf{R}_\kappa\mathbf{d}_\kappa. \tag{15}$$

For small displacements, $\mathbf{d}_\kappa$, the cosine in (14) can be replaced by unity and thus the refinement based on those reflections with l even would result in a pseudo high-temperature structure referred to as the even structure in the following. One expects small displacements $\mathbf{d}_\kappa$ since all critical properties, like the anomaly in birefringence, the shear angle (Ivanov, Tukhtasunov & Shuvalov, 1970), the spontaneous polarization (Shuvalov *et al.*, 1969) and the magnitude of the superlattice intensities are small. The even structure was

---

* Max Planck Institut für Medizinische Forschung, Heidelberg, Federal Republic of Germany.

determined in the first stage of refinement and gave an R factor of 4%. Besides the position $\mathbf{\rho}$, the isotropic Debye–Waller factors and an isotropic extinction coefficient were varied.

In the second stage, including now the odd reflections (superlattice), only the atomic displacements $\mathbf{d}_\kappa$ were fitted. The number of independent displacement vectors $\mathbf{d}_\kappa$ per atom of type K was reduced from eight to two with the symmetry constraint (11). This fit resulted in the already mentioned R factor of 5%.

V. Results and discussion

Strictly speaking, constraint (11) is valid only for infinitesimal displacements $\mathbf{d}_\kappa$. Therefore, it would be desirable to evaluate the validity of the constraints; but the number of parameters would be a factor of four larger and the test requires the collection of more data than obtained in the present experiment. However, as argued above, there is other evidence that the $\mathbf{d}_\kappa$ are small.

Also, if the spontaneous polarization results from a displacement of charges rather than a charge redistribution, then the observed magnitude of 0·013 μC cm^{-2} would correspond to a displacement of only $2{\cdot}6 \times 10^{-3}$ Å along the b axis per molecule. Thus it seems reasonable to make the further assumption that the ferroelectric component of the $\mathbf{d}_\kappa$ can be neglected.

The results of the first stage of refinement are listed in Table 1. They describe the even structure which has the full symmetry of the high-temperature phase. The atomic positions are compared with the results of Tellgren, Ahmad & Liminga (1973) at room temperature. In an unpublished report, which has recently come to our attention, Tellgren & Liminga (1975) have determined the H positions at room temperature with neutron diffraction.

In order to show the main displacements due to the phase transformation the even structure [likewise the results of Tellgren, Ahmad & Liminga (1973) could have been taken] is compared in Table 2 with the results of the second stage of refinement. Atoms labelled by 1 and 6 are related by the symmetry operation $(x + \frac{1}{2}, -y + \frac{1}{2}, -z + \frac{1}{2})$ in the even structure.

The difference between the two structures gives the displacement vectors $\mathbf{D}'_1$ and $\mathbf{D}'_2$ which were introduced in (11). These vectors are listed in Table 3. For the main displacements one finds

$$\mathbf{D}'_1 \simeq \mathbf{D}'_2 \equiv \mathbf{D}. \qquad (16)$$

This observation imposes yet another constraint on the displacements due to the phase transition. This can also be seen from Fig. 1. This figure shows the superposition of the even and the low-temperature structure. The main displacements are depicted by arrows. The arrows for molecule 1 are related to those of molecule 6 by the point operation R_2, in accordance with (16). It must be stressed that this equality is not imposed by the symmetry of the soft mode. That this equality is physically meaningful can be shown by converting the positional changes, shown in Table 2, into bond lengths and angles. Then one sees that the SeO_3 groups remain essentially undistorted by the phase transition. Also, the geometrical point of gravity of the SeO_3 groups does not change during the phase transition. Thus, the main displacements $\mathbf{D}$ of Table 3 (SeO_3 groups with even indices) can be represented by a pure rotation. For the

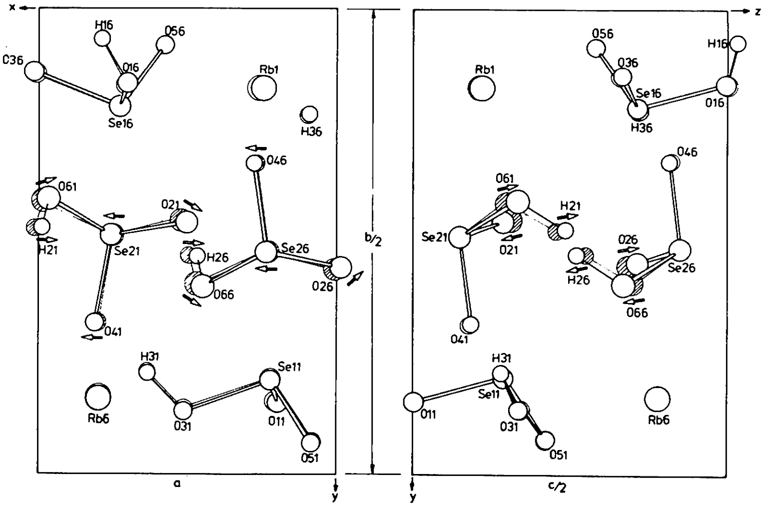

Fig. 1. Superposition of the low-temperature structure and the even structure of $RbH_3(SeO_3)_2$. The arrows show the major displacements due to the phase transition. The shaded atoms represent the even positions. The labelling scheme is as follows: O*κs* denotes the *κ*th oxygen atom created by the *s*th symmetry operation applied to O(1)1 [O1 1], *etc.* For Rb there is no *κ* label.

group around Se(2)1, the rotation angle is calculated to be $-7.1°$ with the rotation axis $\mathbf{N}$ given by

$$\mathbf{N} = (0.1032, 0.9341, 0.3416) \tag{17}$$

which is normalized to unity with the components given in relative units.

It then becomes clear that the displacements of the group of molecule 1 are related to those of molecule 6 *via* the hydrogen bond formed by H(2) (see Fig. 2). The rotations of the other SeO_3 groups can be generated with the eigenvector $\mathbf{e}(1)$ (see equation 11*a*); the results are shown in Fig. 2. It can thus be seen from

Table 1. *Atomic parameters after first stage of refinement*

	x		y		z		
	Even ($\times 10^4$)	Tellgren *et al.* (1973) ($\times 10^5$)	Even ($\times 10^4$)	Tellgren *et al.* (1973) ($\times 10^5$)	Even ($\times 10^4$)	Tellgren *et al.* (1973) ($\times 10^5$)	$\langle U^2 \rangle$ Å^2 ($\times 10^4$)
Se(1)	2143 (4)	21630 (14)	3950 (2)	39527 (4)	1489 (3)	14788 (6)	156 (10)
Se(2)	7311 (3)	73113 (14)	2428 (2)	24215 (4)	828 (4)	8439 (6)	183 (9)
Rb	2646 (4)	26034 (15)	821 (3)	8289 (4)	1157 (3)	11699 (7)	242 (11)
O(1)	1972 (5)	18958 (119)	4193 (4)	42057 (28)	125 (4)	1369 (43)	137 (12)
O(2)	5105 (5)	50635 (98)	2254 (4)	22483 (34)	1610 (6)	15927 (69)	176 (12)
O(3)	4898 (5)	49313 (87)	4286 (4)	42686 (28)	1739 (5)	17033 (51)	128 (15)
O(4)	7742 (5)	77185 (96)	3370 (3)	33470 (24)	973 (5)	9452 (44)	107 (11)
O(5)	733 (5)	8180 (90)	4617 (3)	46152 (28)	2107 (4)	21189 (53)	121 (11)
O(6)	9565 (6)	95210 (96)	2074 (4)	20750 (31)	1564 (6)	16153 (72)	196 (11)
H(1)	2797 (10)		4672 (7)		9953 (8)		267 (14)
H(2)	9821 (11)		2373 (7)		2280 (11)		342 (21)
H(3)	6086 (9)		3896 (8)		1465 (9)		216 (19)
Even	$a = 5.8978$ Å		$b = 17.8350$ Å		$c = 12.4294$ Å		
Tellgren *et al.* (1973)	$a = 5.9192$ Å		$b = 17.9506$ Å		$c = 12.5038$ Å		

Table 2. *Position vectors of molecules* (1) *and* (6) [*see equation* (8)] *in the low-temperature structure and even structure*

Because of the constrained fit [equation (9)], the origin is fixed along the y axis. Molecules 5 and 2 can be found with (9). The remaining four molecules are obtained in the usual way by applying the space-group operations, x,y,z; $\bar{x}, y+\frac{1}{2}, \bar{z}$ of the space group $P2_1$ (C_2^2) after shifting the origin by $(0,0,\pm 1/8)$ where the signs refer to domains 1 and 2 respectively.

	Low-temperature positions $\mathbf{r}_\kappa(K)$			Even-structure positions $R_\kappa\rho(K)$		
	x ($\times 10^4$)	y ($\times 10^4$)	z ($\times 10^4$)	x ($\times 10^4$)	y ($\times 10^4$)	z ($\times 10^4$)
Se(1)1	2202 (3)	3952 (2)	1472 (2)	2143 (4)	3950 (2)	1489 (3)
Se(1)6	−2776 (3)	−8944 (2)	3524 (2)	7143	1050	3511
Se(2)1	7413 (3)	2426 (2)	826 (2)	7311 (3)	2428 (2)	828 (4)
Se(2)6	2435 (3)	−7424 (2)	4174 (2)	12311	2572	4172
Rb1	2644 (3)	829 (2)	1169 (2)	2646 (4)	821 (3)	1157 (3)
Rb2	−2324 (3)	−5826 (2)	3830 (3)	7646	4179	3843
O(1)1	1954 (4)	4195 (3)	121 (3)	1972 (5)	4193 (4)	125 (4)
O(1)6	−2996 (4)	−9197 (3)	4885 (3)	6972	807	4875
O(2)1	5002 (5)	2274 (3)	1474 (5)	5105 (5)	2254 (4)	1610 (6)
O(2)6	−0 (5)	−7280 (3)	3516 (5)	10105	2746	3390
O(3)1	4960 (4)	4297 (3)	1694 (3)	4898 (5)	4286 (4)	1739 (5)
O(3)6	−26 (4)	−9294 (3)	3296 (3)	9898	714	3261
O(4)1	7861 (5)	3366 (3)	993 (3)	7742 (5)	3370 (3)	973 (5)
O(4)6	2892 (5)	−8359 (3)	4009 (3)	12742	1630	4027
O(5)1	803 (4)	4611 (3)	2110 (3)	733 (5)	4617 (3)	2107 (4)
O(5)6	−4187 (4)	−9609 (2)	2891 (3)	5733	383	2893
O(6)1	9440 (6)	2051 (3)	1702 (6)	9565 (6)	2074 (4)	1564 (6)
O(6)6	4445 (6)	−7048 (3)	3304 (5)	14565	2926	3436
H(1)1	2767 (6)	4582 (5)	−53 (6)	2797 (10)	4672 (7)	−47 (8)
H(1)6	−2153 (7)	−9666 (5)	5058 (5)	7797	328	5047
H(2)1	9641 (10)	2362 (6)	2410 (10)	9821 (11)	2373 (7)	2280 (11)
H(2)6	4636 (10)	−7366 (7)	2577 (9)	14821	2627	2720
H(3)1	6141 (6)	3898 (5)	1433 (5)	6086 (9)	2896 (8)	1465 (9)
H(3)6	1147 (7)	−8898 (5)	3555 (5)	11085	1104	3535

Fig. 2 that the phase transition affects only chain (2) leaving chain (1) essentially unchanged. Along chain (2), adjacent SeO_3 groups rotate in opposite senses.

We wish to thank H. Zimmerman for providing the excellent crystals, Drs C. Zeyen and B. Klar for their help with the experiment and data reduction respectively. We also thank Professor H. H. Stiller for his critical reading of the manuscript.

APPENDIX

This Appendix describes the essential steps of the application of the formulation introduced by Maradudin & Vosko (1968) to the present problem, in order to derive the symmetry constraints on the soft-mode eigenvector from (1) and (2) of § II.

To this end one has to find the so-called T matrices which represent the action of a symmetry operation on a displacement field. In the following we adopt the nomenclature of Maradudin & Vosko (1968). The T matrices are defined as

$$T_{\alpha\beta}(\kappa\,\kappa'\,|\,s) = (\mathrm{R}_s)_{\alpha\beta}\,\delta[\kappa, F_0(\kappa',s)] \times \exp\{i\mathbf{k}[\mathbf{x}(\kappa) - \mathrm{R}_s\mathbf{x}(\kappa')]\} \quad (1A)$$

where the sth symmetry operation (R_s denotes its rotational part) of the space group transfers atom κ' into atom $F_0(\kappa', s)$. In our case $F_0(\kappa',s)$ becomes

$$F_0(\kappa', s) = 4 - |5 - (s + \kappa')| - 2\delta_{s\kappa'}(\delta_{2\kappa'} + \delta_{3\kappa'}) \quad (2A)$$

if one associates equation (1) to $\mathbf{x}(\kappa)$. With $\mathbf{k}_{22} = \frac{1}{2}\,\mathbf{c}^*$ now taken for $\mathbf{k}$ the T matrices can be written

$$\left.\begin{array}{l}
\mathrm{T}(1) = \begin{pmatrix} 1 & 0 & 0 & 0 \\ 0 & 1 & 0 & 0 \\ 0 & 0 & 1 & 0 \\ 0 & 0 & 0 & 1 \end{pmatrix} \mathrm{R}_1 \\
\mathrm{T}(2) = \begin{pmatrix} 0 & 1 & 0 & 0 \\ 1 & 0 & 0 & 0 \\ 0 & 0 & 0 & -1 \\ 0 & 0 & -1 & 0 \end{pmatrix} \mathrm{R}_2 \\
\mathrm{T}(3) = \begin{pmatrix} 0 & 0 & i & 0 \\ 0 & 0 & 0 & i \\ i & 0 & 0 & 0 \\ 0 & i & 0 & 0 \end{pmatrix} \mathrm{R}_3 \\
\qquad\quad \kappa \longrightarrow \kappa' \\
\mathrm{T}(4) = \begin{pmatrix} \downarrow 0 & 0 & 0 & -i \\ 0 & 0 & -i & 0 \\ 0 & i & 0 & 0 \\ i & 0 & 0 & 0 \end{pmatrix} \mathrm{R}_4
\end{array}\right\} \quad (3A)$$

Table 3. *Differences between the low-temperature structure [constrained by equation* (11)] *and the even structure*

Figures are given in units of $a, b, c \times 10^4$

	$\mathbf{D}_1'$ from molecule (1)			$\mathbf{D}_2'$ from molecule (6)		
Se(1)	59	2	−17	81	−6	−13
Se(2)	102	−2	−2	124	−4	−2
Rb	−2	8	12	30	5	13
O(1)	−18	2	−4	32	4	−10
O(2)	−103	20	−136	−105	26	−126
O(3)	62	11	−45	76	8	−35
O(4)	119	−4	20	150	−11	18
O(5)	70	−6	3	80	−8	2
O(6)	−125	−23	138	−120	−26	132
H(1)	−30	10	−6	50	−6	−11
H(2)	−180	−11	130	−185	−7	143
H(3)	55	2	−32	61	2	−20

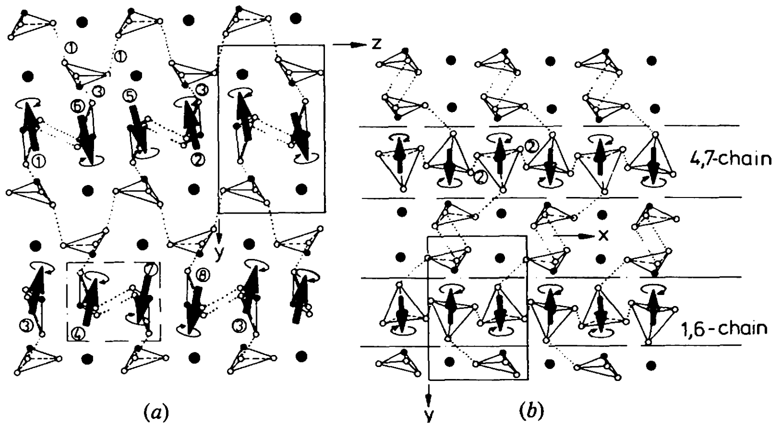

Fig. 2. The mechanism for the creation of the low-temperature phase. The arrows show the axes and sense of rotation of the SeO_3 groups. The sections of Fig. 1 are indicated by frames and represent the projection of a quarter of the low-temperature unit cell. The numbers in circles denote the number of the symmetry operation [equation (8)]. SeO_3 groups linked together by hydrogen bonds ② (dotted lines), thus forming chains running along **x**, are indicated by dashed lines. The dash-dotted frame indicates such a chain in projection along **x**. Interrupted dotted lines (*a*) represent hydrogen bonds, which are connected to SeO_3 groups above and below the figure. That the two modes [see equation (11)] are degenerate can be seen by inversion of the rotation senses of chains 4,7 and 3,8.

where a short notation has been used to represent the 12×12 T matrices. (As already mentioned in § II, one may restrict the symmetry considerations to one atom of the molecule in the present case.)

The T matrices commute with the dynamical matrix and therefore the basis vector $\mathbf{E}(\lambda)$ [see (5)] has to be an eigenvector of the T matrices simultaneously. The matrix $\boldsymbol{\tau}(s)$ of the irreducible representation (2) describes how the vector $\mathbf{E}(\lambda)$ transforms under the action of the T matrices

$$\mathsf{T}(s)\,\mathbf{E}(\lambda) = \sum_{\lambda'=1}^{2} \tau_{\lambda'\lambda}(s)\,\mathbf{E}(\lambda'). \tag{4A}$$

This transformation law gives immediately the symmetry constraints of the basis vector $\mathbf{E}(\lambda)$.

Besides these constraints due to spatial symmetry, there are consequences due to time-reversal symmetry of the dynamical matrix. For $\mathbf{k}$ at the zone boundary, as in the present case, the dynamical matrix becomes real and thus $\mathbf{E}(\lambda)$ may be chosen real and the number of components is halved. Equation (3*A*) shows that $\mathsf{T}(3)$ and $\mathsf{T}(4)$ are imaginary, whereas representation (2) is real. This would lead to complex eigenvectors due to (4*A*). Thus one has to apply an unitary transformation on (2) to arrive at imaginary matrices for $\boldsymbol{\tau}(3)$ and $\boldsymbol{\tau}(4)$. In terms of the Pauli spin matrices this transformation corresponds to a rotation of 90° around the (001) axis. Then we obtain the new representation

$$\begin{array}{c|c|c|c|c} & \mathsf{R}_1 & \mathsf{R}_2 & \mathsf{R}_3 & \mathsf{R}_4 \\ \hline \boldsymbol{\tau}'(s) & \varepsilon & \sigma_z & i\sigma_x & \sigma_y \end{array}. \tag{5A}$$

Insertion now of (5*A*) into (4*A*) gives immediately the basis vectors (6) of § II.

Besides imposing constraints on the basis vectors, time-reversal symmetry can give rise to further degeneracies. For the present problem this is not the case as can be seen by criterion (5.63) of Maradudin & Vosko (1968).

References

Aknazarov, S. K., Shekhtman, V. S. & Shuvalov, L. A. (1974). *Kristallografiya*, **19**, 1291–1292; Engl. trans. (1975). *Sov. Phys. Crystallogr.* **19**, 804–805.

Coppens, P. & Hamilton, W. C. (1970). *Acta Cryst.* A**26**, 71–76.

Fitzgerald, W. J. & Grimm, H. (1977). *Solid State Commun.* **22**, 749–752.

Gesi, K., Ozawa, K. & Makita, Y. (1973). *Jpn. J. Appl. Phys.* **12**, 1963–1964.

Grimm, H. & Fitzgerald, W. J. (1978). To be published.

ILL (1974). *Neutron Research Facilities at the High-Flux Reactor of the ILL*. Institut Laue–Langevin. BP 156X. 38042 Grenoble CEDEX, France.

Ivanov, N. R., Tukhtasunov, I. T. & Shuvalov, L. A. (1970). *Kristallografiya*, **15**, 752–755; Engl. trans. (1971). *Sov. Phys. Crystallogr.* **15**, 647–650.

Klar, B. (1975). Internal Report 75K18T. Institut Laue Langevin, BP 156X, 38042 Grenoble CEDEX, France.

Kovalev, O. V. (1965). *Irreducible Representations of the Space Groups*. New York: Gordon and Breach.

Levanyuk, A. P. & Sannikov, D. G. (1970). *Fiz. Tverd. Tela (Leningrad)*, **12**, 2997–3000; Engl. trans. (1971). *Sov. Phys. Solid State*, **12**, 1418–1421.

Makita, Y. & Suzuki, S. (1974). *J. Phys. Soc. Jpn*, **36**, 1215.

Maradudin, A. A. & Vosko, S. H. (1968). *Rev. Mod. Phys.* **40**, 1–37.

Shuvalov, L. A., Ivanov, N. R., Gordeyeva, N. V. & Kirpichnikova, L. F. (1969). *Kristallografiya*, **14**, 658–662; Engl. trans. (1970). *Sov. Phys. Crystallogr.* **14**, 554–558.

Shuvalov, L. A., Ivanov, N. R., Gordeyeva, N. V. & Kirpichnikova, L. F. (1970). *Phys. Lett. A*, **33**, 490–491.

Tellgren, R., Ahmad, D. & Liminga, R. (1973). *J. Solid State Chem.* **6**, 250–259.

Tellgren, R. & Liminga, R. (1975). Report UUIC-B19-130. Uppsala Univ., Sweden.

Tovbis, A. B., Davydova, T. S. & Simonov, V. I. (1972). *Kristallografiya*, **17**, 103–106; Engl. trans. (1972). *Sov. Phys. Crystallogr.* **17**, 81–84.